Catalysis Today 166 (2011) 18–24

Contents lists available at ScienceDirect

Catalysis Today

journal homepage: www.elsevier.com/locate/cattod

Generation of highly reactive OH groups at the surface of TiO_2 nanotubes

A. Rendón-Rivera, J.A. Toledo-Antonio*, M.A. Cortés-Jácome, C. Angeles-Chávez

Instituto Mexicano del Petróleo, Eje Central Lázaro Cárdenas 152, Col. San Bartolo Atepehuacan, 07730 México, D.F., Mexico

ARTICLE INFO

Article history:
Available online 24 April 2010

Keywords:
Titania nanotubes
FTIR CO adsorption
Raman spectroscopy
Transmission electron
Microscopy

ABSTRACT

Titania with nanotubular morphology was synthesized hydrothermally via the reaction of a commercial TiO_2 anatase with NaOH solution at 413 K followed by a washing procedure with an HCl solution. The obtained nanotubes were dried at 373 K and then annealed at 573 and 673 K. All samples were characterized using X-ray diffraction, Raman spectroscopy, HRTEM, nitrogen physisorption and FTIR of adsorbed CO. Tubular morphology was preserved up to 673 K although the collapse of nanotube walls took place and formation of anatase microdomains was observed. Low temperature CO adsorption was followed by FTIR on orthorhombic layered titanate and on anatase transformed nanotubes. The samples were annealed in situ and ex situ in order to know the origin of reactivity of surface OH groups. In situ treated samples presented higher adsorption of CO molecules than samples treated ex situ, nevertheless, the latter present higher activity toward CO oxidation into CO_2. FTIR results reveal the existence of highly reactive OH groups toward CO oxidation at the surface of nanotubular titania calcined ex situ. These hydroxyl groups might be generated from the dissociation of water molecules adsorbed on the strongly deformed TiO_6 octahedra in the curved structure of nanotubes. This fact suggests that enhancement of CO oxidation activity of TiO_2 nanotubes can be achieved by their exposure to adequate doses of water vapor, producing CO_2 at temperatures as low as 100 K. Total extinction of CO and CO_2 vibration bands in FTIR spectra at temperatures above 240 K evidenced the reversibility of the adsorption process.

1. Introduction

Titanium oxide is one of the most studied metal oxides because of its remarkable characteristics (non-toxicity, inertness, chemical and thermal stability, high refractive index) in multiple and different applications. TiO_2 has been used in the construction of solar cells [1,2], as gas sensors [3,4], as photocatalysts [5–8], in the degradation and adsorption processes of organic molecules [5,7,9,10], in heterogeneous catalysis [11,12], as a pigment [13], as anode material for lithium–ion batteries [14,15], etc. With the emergence of nanotechnology much research has been done in order to synthesize nanostructured materials, including those based on metal oxides that show new and improved properties. Different methodologies have been employed for the synthesis of nanotubes, nanoparticles, nanorods, nanobelts of several transition metal oxides. Particularly, nanotubular form of titanium oxide is relative easy to synthesize [16] and is especially interesting, since it combines versatile chemical behavior with high-aspect-ratio and high specific surface area. Titania nanotubes present enhanced properties like photo and catalytic activity, optoelectronic characteristics [17], enhanced energy conversion efficiencies in dye-sensitized solar cells [2], among others.

Although several properties of TiO_2 nanotubes have been exploited for new uses, lack of knowledge exist about its surface chemistry. In order to study the nature and abundance of surface sites on metal oxides, adsorption of different probe molecules can be carried out. Carbon monoxide is one of the most used probe molecules for the characterization of Lewis and Brønsted acidic and basic sites; it also can provide information about the coordination and oxidation state of atoms. The adsorption of CO on TiO_2 surface evidenced the existence of three different sites of interaction: OH groups, Ti^{n+} and basic oxygens [18–21].

For tetragonal anatase phase, the adsorption of CO at low temperature leads to the formation of carbonyls on different Ti^{4+} sites [18]. The most energetic site (α-site) is characterized by a band at 2210 cm^{-1}, a less energetic site (β′-site) is represented by a band at 2192 cm^{-1}. A third kind of Ti^{4+} sites (β″-site) interact with CO molecules preadsorbed on β′-sites generating a common band whose maximum is shifted to 2179 cm^{-1} at higher coverage. In addition to the aforementioned bands, an extra band is formed at 2165 cm^{-1}, which stand for sites designated as γ-sites [18]. In the case of rutile, the existence of one band at 2193 cm^{-1} (α-sites) is reported; with the increase of CO coverage, this band shifts its maximum to 2183 cm^{-1} (β′-sites) [19]. Carbon monoxide and OH groups situated on TiO_2 surface interact forming a hydrogen bond. CO adsorbed on hydroxyl groups of rutile surface generates a band

* Corresponding author. Tel.: +52 55 91 75 8433.
E-mail addresses: rradrian@imp.mx (A. Rendón-Rivera), jtoledo@imp.mx (J.A. Toledo-Antonio).

0920-5861/$ – see front matter © 2010 Elsevier B.V. All rights reserved.
doi:10.1016/j.cattod.2010.03.045

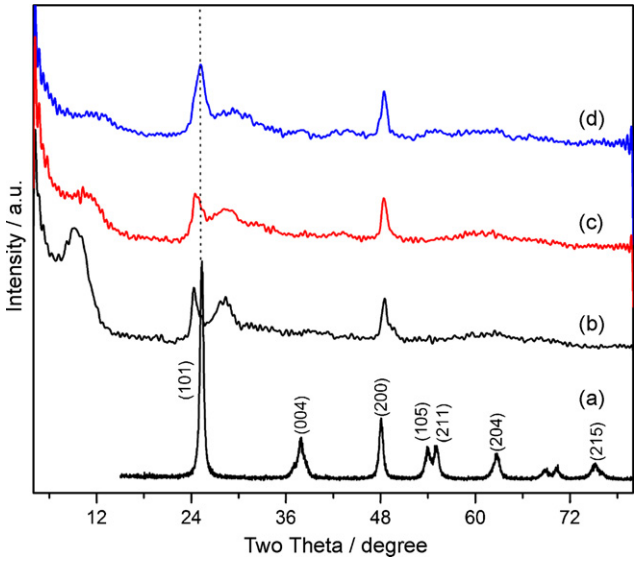

Fig. 1. XRD patterns of (a) anatase TiO_2 used as precursor and TiO_2 nanotubes annealed at: (b) 373 K, (c) 573 K, and (d) 673 K.

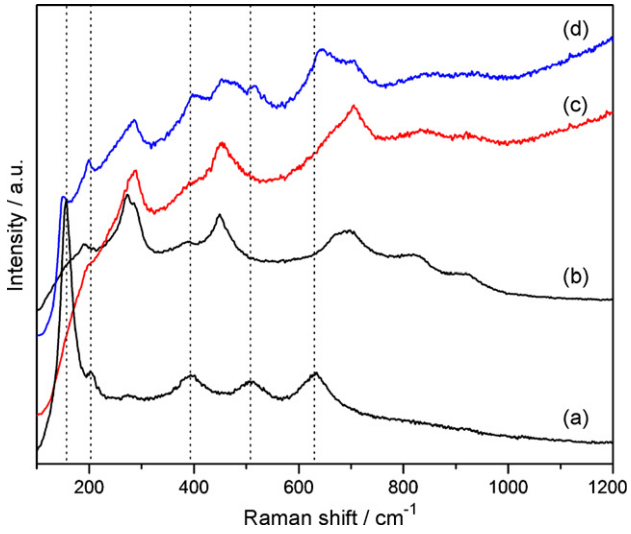

Fig. 2. Raman spectra of (a) anatase TiO_2 used as precursor and TiO_2 nanotubes annealed at: (b) 373 K, (c) 573 K, and (d) 673 K.

at 2150 cm^{-1} [19], whereas on anatase is located at 2155 cm^{-1} [18]. Physically adsorbed CO produced bands in the 2148–2133 cm^{-1} region due to its interaction with O^{2-} surface anions [20].

Recently, it was reported a FTIR study of CO adsorption at low temperature on titania nanotubes annealed ex situ at 573 and 673 K [22]. Almost the complete transformation of the orthorhombic structure of the synthesized nanotubes into anatase was observed in samples annealed at 673 K. The adsorbed CO species react via surface with OH groups in the anatase curved structure of nanotubes, yielding CO_2 and H_2O at 183 K. The CO_2 thus produced remained adsorbed and reacted in turn with other surface OH groups producing carbonates and H_2O. The carbonate species were eliminated at high temperature (473 K), restoring the surface OH groups and producing gaseous CO_2.

In this work, the origin of the reactivity of OH groups at the surface of titanate nanotubes toward CO oxidation was studied by FTIR of CO adsorption on in situ and ex situ annealed samples at 573 and 673 K. The OH groups of ex situ annealed sample exhibited superior reactivity toward the oxidation of CO into CO_2.

2. Experimental details

Titania with nanotubular morphology was synthesized by hydrothermal treatment of an anatase precursor with a crystallite size of 20 nm (as determined by XRD Rietveld refinement analysis) Hombikat KO3. Nineteen grams of anatase powder were suspended in 425 mL of an aqueous NaOH 10 M solution, the resulting suspension was placed and sealed in a 500 mL autoclave. The hydrothermal reaction was conducted at 413 K for 24 h under stirring at 200 rpm. The resultant white slurry was filtered and neutralized with 1 M HCl solution until the pH was 3.0. Thereafter, the obtained suspension was stirred overnight. The material was repeatedly washed with abundant deionized water until it was chlorine-free. Finally the material was dried at 373 K, yielding a hydrous titania powder with nanotubular morphology. A fraction of dried material was annealed at 573 and 673 K under dynamic nitrogen flow in a tubular oven for 3 h and other amount was preserved for activation inside the cell of IR equipment.

X-ray diffraction (XRD) patterns of the samples packed in a glass holder were recorded at room temperature with Cu Kα radiation in a Bruker Advance D-8 diffractometer having theta–theta configuration and a graphite secondary-beam monochromator. The data were collected for scattering angles (2θ) ranging from 4° to 80° with a step of 0.02° for 2 s per point.

High-resolution transmission electron microscopy (HRTEM) analyses of the samples were performed in a JEOL 2010F microscope operating at 200 kV and equipped with a Schottky-type field emission gun and an ultrahigh resolution pole piece (Cs = 0.5 mm, point-to-point resolution, 0.190 nm). The samples were ground, suspended in isopropanol at room temperature and dispersed by ultrasonic agitation. Then, an aliquot of the solution was dropped on a 3 mm diameter lacey carbon copper grid.

The Raman spectra were recorded using an Yvon Jobin Horiba (T64000) spectrometer, equipped with a confocal microscope (Olympus, BX41) with an argon ion laser operating at 514.5 nm at a power level of 10 mW. The spectrometer was equipped with a CCD camera detector. Powdered titania nanotubes were placed in a Linkam cell stage directly adapted to the microscope of the instrument, which provides a controlled atmosphere and temperature. The glass window of the cell was 1 mm thick.

All textural properties were determined in an ASAP-2000 analyzer from Micromeritics. The specific surface area was calculated from the Brunauer–Emmet–Teller (BET) equation from N_2 physisorption at 77 K. The pore size distribution was obtained by the Barrett–Joyner–Halenda (BJH) method from the desorption branch. Dried and annealed samples were outgassed at 373 K.

Transmission infrared (IR) spectra were recorded using a Nicolet Fourier transform infrared (FTIR) spectrophotometer at a spectral resolution of 4 cm^{-1} accumulating 100 scans, in a self-supported disk. The IR cell was connected to a vacuum/sorption system capable of temperature control with a <0.133 Pa residual pressure. The cell allowed recording the IR spectra at 100 K. Self-supported disks of the samples annealed ex situ at 573 and 673 K were outgassed under vacuum at 573 K before exposing them to CO. Other self-supported disks were thermally treated into the IR cell under nitrogen flow at 573 and 673 K respectively (in situ annealed samples) before exposing them to CO. The adsorption procedure consisted in contacting the annealed sample disk with CO at 100 K at a pressure of 5.3 kPa in the IR cell where the spectrum of the adsorption was recorded. The IR cell was cooled with liquid nitrogen. Then, desorption was carried out by outgassing upon heating from 100 K to room temperature. FTIR spectra were recorded at each 10 K.

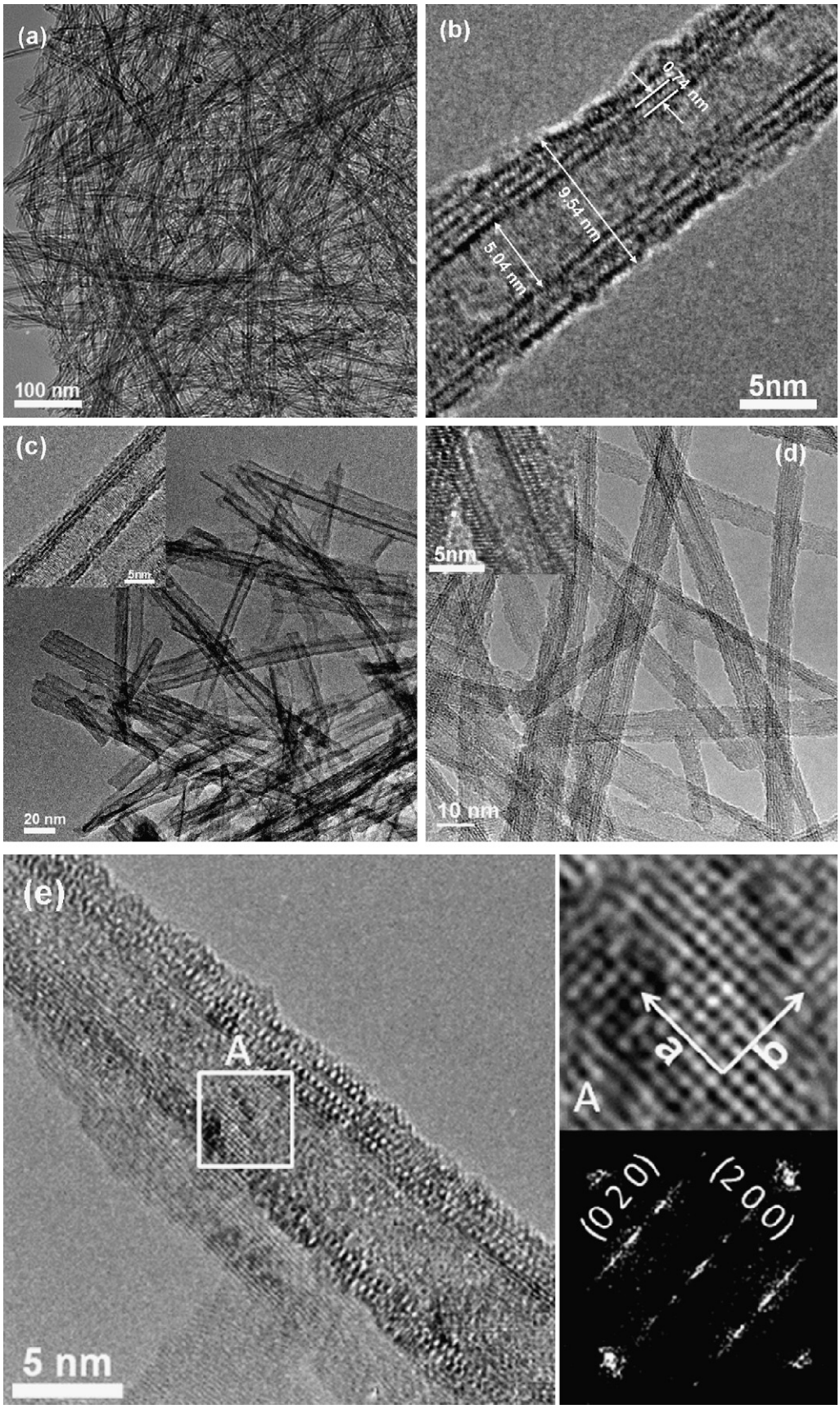

Fig. 3. TEM images showing synthesized titania nanotubes annealed at: (a and b) 373 K, (c) 573 K, and (d and e) 673 K.

3. Results and discussion

Fig. 1(a) shows the XRD pattern of TiO_2 anatase powder used as the raw material. The crystallite size of the anatase precursor was around 20 nm, and its specific surface area was 101 m^2/g determined by the BET method. Titania nanotubes were prepared by alkaline hydrothermal treatment of anatase at 413 K and then the as obtained material was dried at 373 K, its XRD pattern exhibited four broad peaks at $2\theta = 9.2^\circ$, 24.3°, 28.3°, and 48.5°, as shown in Fig. 1(b). XRD peaks do not correspond to anatase phase indicating complete transformation into an orthorhombic structure of layered hydrogen titanates, $H_2Ti_2O_4(OH)_2$ as previously reported [23,24]. At 573 K, the XRD pattern does not showed changes indicating preservation of the orthorhombic structure. After annealing at 673 K, the XRD peak at 9.2° disappeared, as well as the peak at 28.3°. The peak at 24.3° originally present in the titania nanotubes, slightly shifted to 25.3°, the position of the (1 0 1) plane in anatase phase, as indicated in Fig. 1. These results evidenced the collapse of the nanotube walls and the structure reconversion to tetragonal anatase.

In addition to Raman spectra of titania nanotubes, the one corresponding to anatase precursor was included in Fig. 2(a), it exhibited five bands at 156, 205, 397, 511, and 636 cm^{-1}. Fig. 2(b) shows the spectra for nanotubular titanates dried at 373 K, it present three major bands at 280, 449, and 687 cm^{-1} and other weak bands at 190, 389, 825, and 922 cm^{-1}, all these bands are different from those of anatase phase and their exact assignment is still not available but several attempts had been made by many groups [23,25–31]. According to the literature, bands at 450 and 668 cm^{-1} could be assigned to Ti–O–Ti vibrations [31], however in our Raman spectra the band at 668 cm^{-1} is shifted to 687 cm^{-1}. A band in the range of 822–830 cm^{-1} was related to a covalent Ti–O–H bond [26] and the band at 917 cm^{-1} was attributed to Ti–O–Na vibrations [31]. Low concentration of Na^+ ions in our nanotubes could have originated a very weak vibration band at 922 cm^{-1} but this band could also be attributed to Ti–O–H bonds generated during extensive ion exchange carried out in neutralization process with HCl [23]. After annealing at 573 K, the intensity of some Raman vibrations of nanotubes considerably decrease but no clear detection of anatase peaks was made. Associating this result with the one obtained by XRD (Fig. 1(c)), it can be confirmed the titanate nanotubes structure stability up to 573 K. On the other hand, the spectrum of annealed nanotubes at 673 K exhibited the presence of anatase active modes at 152, 401, 515, 640 cm^{-1}, although the main peaks corresponding to titanate nanotubes structure were still be observed at 287, 452, and 703 cm^{-1}. The coexistence of these two TiO_2 phases is related to a transformation of the titanate nanotubular structure into anatase probably caused by collapse of layered arrangement and subsequent microdomain formation of the latter, in agreement with XRD results.

TEM micrograph of the as obtained material (Fig. 3(a)) reveals tube-like nanostructures with lengths in the range of micrometers. No raw anatase nanoparticles were observed indicating that all the initial material was transformed into nanotubes. Fig. 3(b) shows that the number of nanotubes walls counted from the two sides is not identical as 2–4 layers. The distance between adjacent structural layers is about 0.74 nm, the inner and outer diameters of titania nanotubes were about 5 and 10 nm respectively. After heat treatment at 573 K, the nanotubular morphology was preserved although its length decreased as showed in Fig. 3(c). Similar morphological stability was observed for samples annealed at 673 K (Fig. 3(d)) although the layered structures began to collapse bringing about the extinction of the space between nanotube walls and producing microdomains of anatase nanocrystals as seen in Fig. 3(e). The white square marked as A surrounds the Fourier transformed region of the titania nanotube where anatase nanocrystals

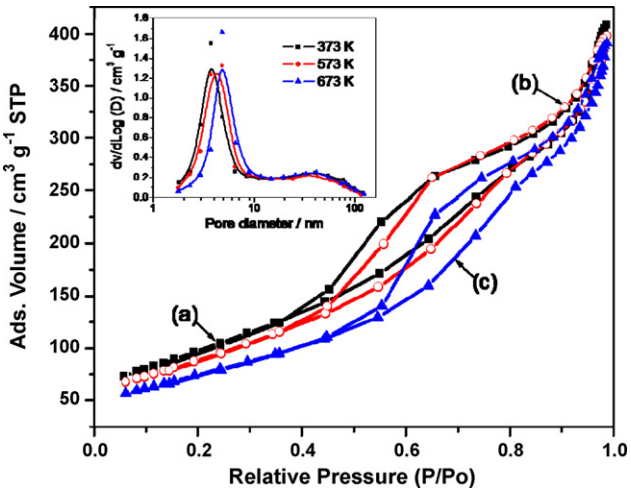

Fig. 4. Nitrogen adsorption–desorption isotherms for annealed nanotubes at: (a) 373 K, (b) 573 K, and (c) 673 K. Corresponding pore size distribution plots are shown in the inset.

were observed. The FFT pattern of A region shows characteristic spots with a *d*-spacing of 0.189 nm, named as (2 0 0) anatase planes, these planes represent a half of the unit cell in the *a*-axis, therefore parameter *a* is approximately 0.378 nm. The same interplanar spacing was observed between spots that are situated in a perpendicular position respect to the ones that represent (2 0 0) planes. Then, perpendicular spots are named as (0 2 0) anatase planes and they represent half of the unit cell in the *b*-axis, this way parameter *b* is approximately the same length as *a*.

Annealing treatment brings about phase transition from titanate nanotubular structure into anatase, modifying textural properties. N_2 adsorption–desorption isotherms of TiO_2 nanotubes treated in nitrogen atmosphere at 373, 573, and 673 K are shown in Fig. 4. The aforementioned isotherms are of classical type IV, characteristic of mesoporous materials according to the IUPAC classification [32]. The three isotherms presented a similar shape but the hysteresis loop shifted toward higher relative pressure with the increment of annealing temperature. This suggests a slight enhancement in the internal porosity of nanotubes. The inset in Fig. 4 shows the pore-size distribution plots determined from the desorption branch of the isotherm. The peak around 4–5 nm correspond to the inner diameter of nanotubes, in agreement with the inner diameter measured in HRTEM images (Fig. 3(b)). The other broad peak in the range of 15–100 nm is likely to arise from the aggregation and intercrossing of nanotubes that generated non-uniform interparticle voids. Textural parameters listed in Table 1 show an increase in the average pore diameter from 5.0 to 6.2 nm and a minor decrement in total pore volume from 0.65 to 0.61 $cm^3\ g^{-1}$, when the annealing temperature increased from 373 to 673 K. After annealing at 573 K, pore diameter and pore volume did not vary considerably in comparison with those of titanate nanotubes dried at 373 K, indicating that the nanotubular morphology was still preserved in full agreement with Raman and XRD results. On the other hand, after annealing at 673 K, the pore diameter increased up to 6.2 nm with a slight pore volume variation, then, pore size increase could be

Table 1
Textural properties of titania nanotubes annealed at indicated temperatures.

Temperature (K)	Specific surface area ($m^2\ g^{-1}$)	Total pore volume ($cm^3\ g^{-1}$)	Average pore diameter (nm)
373	353	0.65	5.0
573	320	0.63	5.2
673	270	0.61	6.2

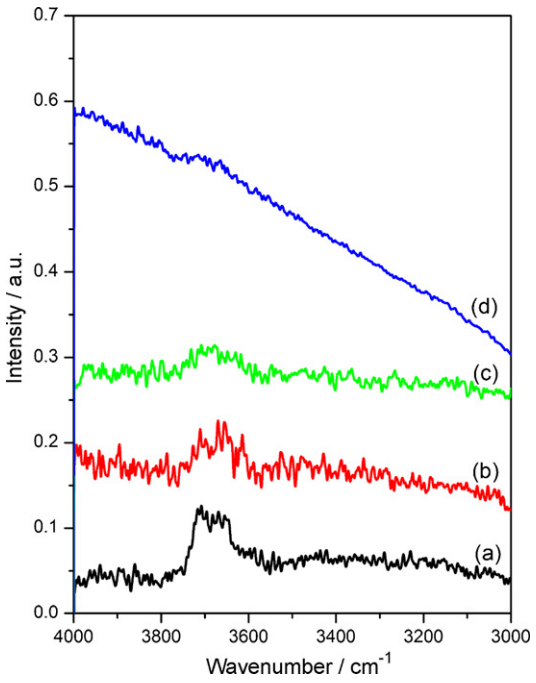

Fig. 5. FTIR spectra of titania nanotubes annealed in situ at: (a) 573 K and (c) 673 K and ex situ at: (b) 573 K and (d) 673 K.

explained by the collapse of the layers of the nanotubes walls, this fact also explained the decrement in specific surface area from 353 to 270 $m^2\ g^{-1}$.

Fig. 5 shows FTIR spectra at the OH regions of titania nanotubes after in situ and ex situ treatments in nitrogen at 573 and 673 K. These spectra exhibited a weak vibration band in the ν(OH) region at around 3700 cm^{-1} which correspond to highly basic OH^- groups on nanotubes in terminal positions [33]. As all the spectra were normalized to the same sample weight, the low intensity of ν(OH) band in ex situ treated samples suggests lower concentration of OH groups than in situ treated ones.

The FTIR spectra of CO adsorption on the orthorhombic structure of the titanate nanotubes, $H_2Ti_2O_4(OH)_2$, annealed in situ at 573 K are shown in Fig. 6(a). At 100 K, CO adsorption gives rise to a band at 2163 cm^{-1}, this band has been attributed to the CO adsorption on surface Ti–OH groups since a shift of the band characterizing surface hydroxyl groups occurred simultaneously [18,34–36]. Also a shoulder is presented at 2142 cm^{-1}, that can be attributed to physisorbed CO on O^{2-} anions [20]. The band assigned to CO adsorbed on OH surface groups is observed for the TiO_2 nanotubes annealed in situ at 673 K and for the ones annealed ex situ at the same temperatures even though structural transformation started at 673 K (Fig. 7). A blue shift is distinguished for this band with the increment of the evacuation temperature for all samples. During desorption of CO, a new vibration band appeared in the range of 2346–2352 cm^{-1} for all nanotubular samples which is attributed to physisorbed CO_2 species [37]. Carbon monoxide strongly adsorbed on the surface of the titania nanotubes was oxidized by the reaction with surface hydroxyl groups forming CO_2 [22]. For the sample treated in situ at 573 K the CO_2 vibration band appeared at an evacuation temperature of 170 K, meanwhile for the sample annealed ex situ, the CO_2 vibration peak appear at 150 K, suggesting more reactive surface OH groups on ex situ annealed nanotubes. The same behavior was observed for samples treated in situ and ex situ at 673 K; the sample annealed in situ exhibited a CO_2 vibration band starting at 170 K and the sample annealed ex situ exhibited a CO_2 vibration band at temperatures as low as 100 K. The appearance of CO_2 vibration bands at lower temperatures for ex situ treated samples

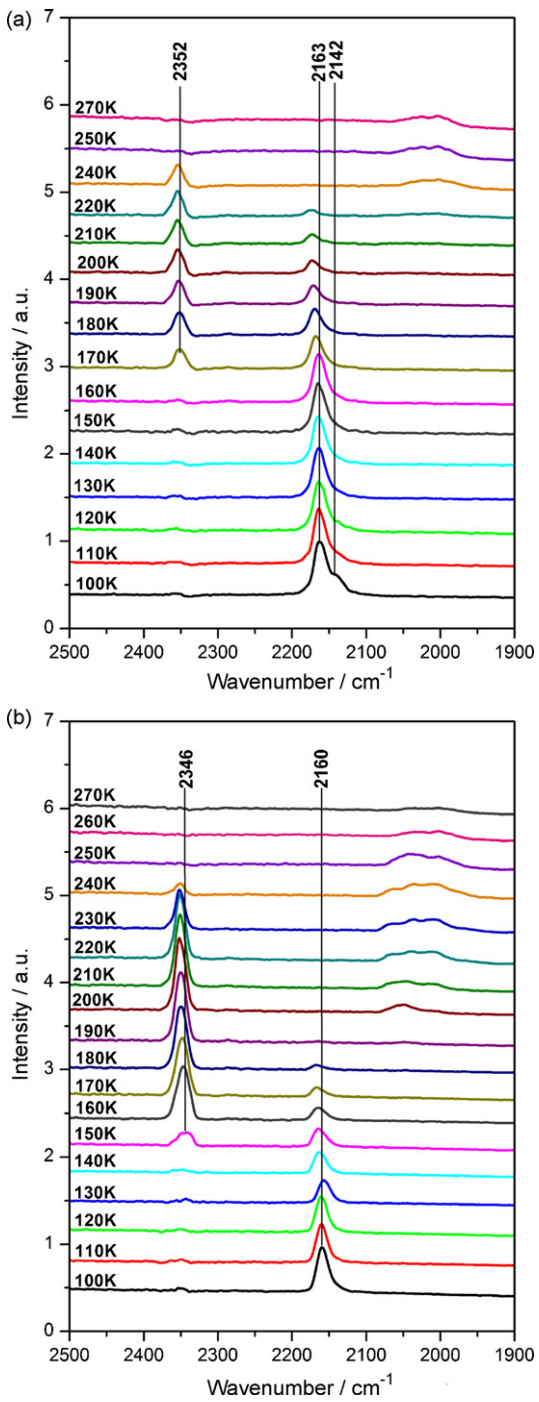

Fig. 6. FTIR spectra of titania nanotubes annealed at 573 K: (a) in situ and (b) ex situ.

suggests the existence of more active sites toward oxidation. For desorption temperatures above 240 K, the IR spectra showed the completely extinction of bands corresponding to adsorbed CO and CO_2.

As all FTIR spectra were normalized to the same sample weight the integrated area of each vibration peak represent the amount of each adsorbed component. Fig. 8 plots the total area corresponding to the CO adsorption band around 2163 cm^{-1} versus the evacuation temperature. It shows maximum area values for samples annealed in situ, this result suggests that in situ treated nanotubes have a higher density of CO adsorption sites (hydroxyl groups), which is in agreement with the intensity trends of OH signal observed in the in situ treated samples before CO adsorption. Fig. 9 shows

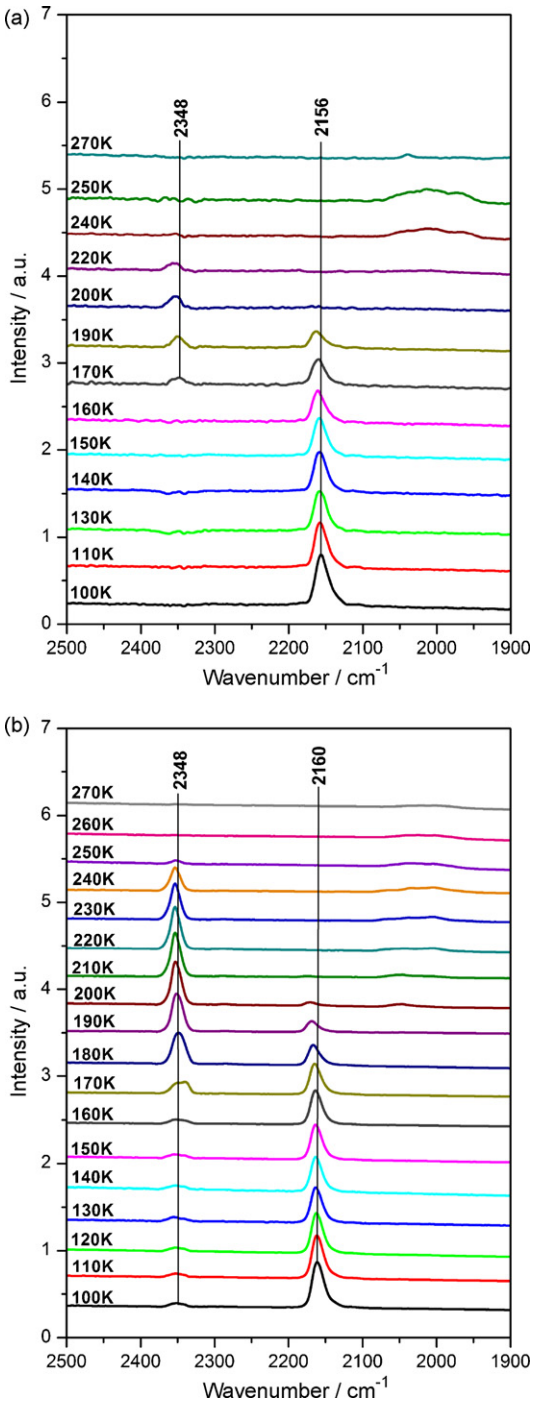

Fig. 7. FTIR spectra of titania nanotubes annealed at 673 K: (a) in situ and (b) ex situ.

the area variation of the band corresponding to adsorbed CO_2 versus the increment of the evacuation temperature. The adsorbed amounts of CO_2, as in the case of CO, are directly related with the integrated area of the corresponding bands. The highest area value corresponds to the nanotubes treated ex situ at 573 K. At this temperature orthorhombic structure of hydrogen titanate was observed for both in situ and ex situ treated samples, then, it can be established that the reactivity of OH groups is independent of the structure of the nanotubes. Therefore it is suggested that the origin of the highly reactive OH groups came from the dissociation of water molecules that were adsorbed on the strongly deformed TiO_6 octahedra in the curved structure of nanotubes.

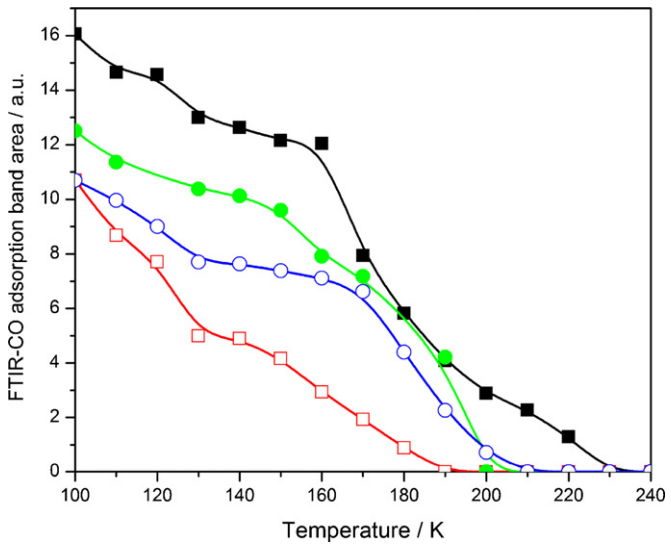

Fig. 8. Variation of the area of the CO adsorption bands for samples treated in situ at 573 K (■), ex situ at 573 K (□), in situ at 673 K (●) and ex situ at 673 K (○) with evacuation temperature.

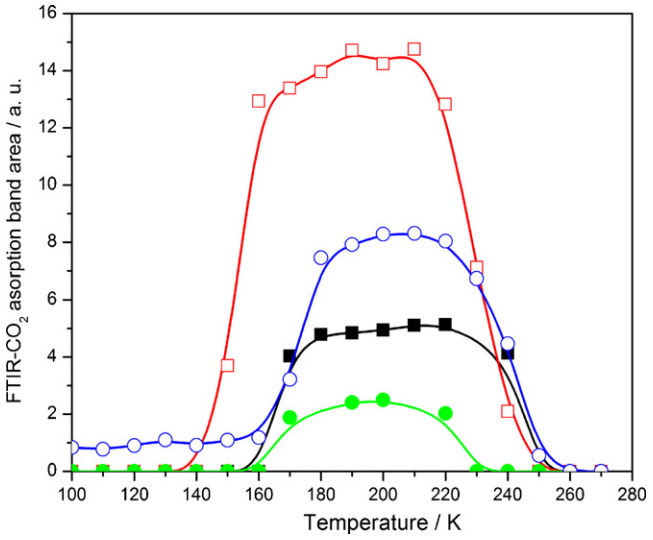

Fig. 9. Variation of the area of the CO_2 adsorption bands for samples treated in situ at 573 K (■), ex situ at 573 K (□), in situ at 673 K (●) and ex situ at 673 K (○) with evacuation temperature.

4. Conclusion

Commercial TiO_2 anatase was transformed into titanate nanotubes after an alkaline hydrothermal treatment at 413 K. Morphological stability was observed for annealed nanotubular titania at 573 and 673 K although at the latter temperature the titanate layered structures began to collapse producing microdomains of anatase. Textural properties also were modified with heat treatments nevertheless they maintain acceptable values. FTIR spectra of the CO adsorption on titanate nanotubes annealed in situ and ex situ revealed the existence of OH groups with different adsorption an oxidation capacity. In situ treated nanotubes exhibited higher CO adsorption capacity meanwhile ex situ treated samples presented higher activity toward CO oxidation into CO_2. The more reactive OH groups of ex situ annealed samples might be generated from the dissociation of water molecules adsorbed from ambient atmosphere on strongly deformed TiO_6 octahedra in the curved structure of nanotubes. The OH reactivity is independent of the

crystallographic structure of titania nanotubes but it depends on the nanotubular morphology. Then, the exposure of nanotubular titania to adequate doses of water vapor can strongly enhance its CO oxidation activity producing CO_2 at temperatures as low as 100 K. At temperatures above 240 K completely extinction of CO and CO_2 bands was observed suggesting the reversibility of the adsorption process.

This highly oxidation activity opens the possibility of potential uses for TiO_2 nanotubes, since the conversion of CO at low temperature is widely applied, like in air cleaning, gas masks for mining applications, CO detectors [38].

Acknowledgements

The authors thank Instituto Mexicano del Petroleo for its financial support under the projects D.00446 and Q.00013.02.053. A. Rendon-Rivera also thanks CONACyT for the Ph.D scholarship.

References

[1] S.I. Na, S.S. Kim, W.K. Hong, J.W. Park, J. Jo, Y.C. Nah, T. Lee, D.Y. Kim, Electrochim. Acta 53 (2008) 2560.
[2] D.J. Yang, H. Park, S.J. Cho, H.G. Kim, W.Y. Choi, J. Phys. Chem. Solids 69 (2008) 1272.
[3] F. Siviero, N. Coppedè, A. Pallaoro, A.M. Taurino, T. Toccoli, P. Siciliano, S. Iannotta, Sens. Actuators B 126 (2007) 214.
[4] M. Gerlich, S. Kornely, M. Fleischer, H. Meixner, R. Kassing, Sens. Actuators B 93 (2003) 503.
[5] M. Katoh, H. Aihara, T. Horikawa, T. Tomida, J. Colloid Interface Sci. 298 (2006) 805.
[6] A.R. Liu, S.M. Wang, Y.R. Zhao, Z. Zheng, Mater. Chem. Phys. 99 (2006) 131.
[7] M.C. Hidalgo, M. Aguilar, M. Maicu, J.A. Navío, G. Colón, Catal. Today 129 (2007) 50.
[8] S. Bakardjieva, J. Šubrt, V. Štengl, M.J. Dianez, M.J. Sayagues, Appl. Catal. B 58 (2005) 193.
[9] C.K. Lee, S.S. Liu, L.C. Juang, C.C. Wang, M.D. Lyu, S.H. Hung, J. Hazard. Mater. 148 (2007) 756.
[10] A.J. Maira, K.L. Yeung, J. Soria, J.M. Coronado, C. Belver, C.Y. Lee, V. Augugliaro, Appl. Catal. B 29 (2001) 327.
[11] J. Escobar, J.A. Toledo, M.A. Cortés, M.L. Mosqueira, V. Pérez, G. Ferrat, E. López-Salinas, E. Torres-García, Catal. Today 106 (2005) 222.
[12] M.A. Cortes-Jácome, M. Morales, C. Angeles Chavez, L.F. Ramírez-Verduzco, E. López-Salinas, J.A. Toledo-Antonio, Chem. Mater. 19 (2007) 6605.
[13] S. Kanti Biswas, D. Dhak, A. Pathak, P. Pramanik, Mater. Res. Bull. 43 (2008) 665.
[14] M. Hibino, K. Abe, M. Mochizuki, M. Miyayama, J. Power Sources 126 (2004) 139.
[15] L.J. Fu, H. Liu, H.P. Zhang, C. Li, T. Zhang, Y.P. Wu, R. Holze, H.Q. Wu, Electrochem. Commun. 8 (2006) 1.
[16] T. Kasuga, M. Hiramatsu, A. Hoson, T. Sekino, K. Niihara, Adv. Mater. 11 (1999) 1307.
[17] M. Alam Khan, H.T. Jung, O.B. Yang, Chem. Phys. Lett. 458 (2008) 134.
[18] K. Hadjiivanov, J. Lamotte, J.C. Lavalley, Langmuir 13 (1997) 3374.
[19] K. Hadjiivanov, Appl. Surf. Sci. 135 (1998) 331.
[20] K. Hadjiivanov, A. Penkova, M.A. Centeno, Catal. Commun. 8 (2007) 1715.
[21] J.C. Lavalley, Catal. Today 27 (1996) 377.
[22] J.A. Toledo-Antonio, S. Capula, M.A. Cortés-Jácome, C. Angeles-Chávez, E. López-Salinas, G. Ferrat, J. Navarrete, J. Escobar, J. Phys. Chem. C 111 (2007) 10799.
[23] M.A. Cortés-Jácome, G. Ferrat-Torres, L.F. Flores Ortiz, C. Angeles-Chávez, E. López-Salinas, J. Escobar, M.L. Mosqueira, J.A. Toledo-Antonio, Catal. Today 126 (2007) 248.
[24] J. Yang, Z. Jin, X. Wang, W. Li, J. Zhang, S. Zhang, X. Guo, Z. Zhang, Dalton Trans. (2003) 3898.
[25] R. Ma, K. Fukuda, T. Sasaki, M. Osada, Y. Bando, J. Phys. Chem. B 109 (2005) 6210.
[26] L. Qian, Z.L. Du, S.Y. Yang, Z.S. Jin, J. Mol. Struct. 749 (2005) 103.
[27] X. Sun, Y. Li, Chem. Eur. J. 9 (2003) 2229.
[28] B.D. Yao, Y.F. Chan, X.Y. Zhang, W.F. Zhang, Z.Y. Yang, N. Wang, Appl. Phys. Lett. 82 (2003) 281.
[29] Á. Kukovecz, M. Hodos, Z. Kónya, I. Kiricsi, Chem. Phys. Lett. 411 (2005) 445.
[30] M. Hodos, E. Horváth, H. Haspel, Á. Kukovecz, Z. Kónya, I. Kiricsi, Chem. Phys. Lett. 399 (2004) 512.
[31] D.V. Bavykin, J.M. Friedrich, A.A. Lapkin, F.C. Walsh, Chem. Mater. 18 (2006) 1124.
[32] K.S.W. Sing, D.H. Everett, R.A.W. Haul, L. Moscou, R.A. Pierotti, J. Rouquérol, T. Siemieniewska, Pure Appl. Chem. 57 (1985) 603.
[33] C. Pazé, S. Bordiga, C. Lamberti, M. Salvalaggio, A. Zecchina, G. Bellussi, J. Phys. Chem. B 101 (1997) 4740.
[34] K. Hadjiivanov, B.M. Reddy, H. Knözinger, Appl. Catal. A 188 (1999) 355.
[35] A. Zecchina, C. Lamberti, S. Bordiga, Catal. Today 41 (1998) 169.
[36] J.A. Toledo-Antonio, M.A. Cortés-Jácome, J. Navarrete, C. Angeles-Chavez, E. López-Salinas, A. Rendon-Rivera, Catal. Today, in press, doi:10.1016/j.cattod.2009.11.011.
[37] Z.H. Cheng, A. Yasukawa, K. Kandori, T. Ishikawa, Langmuir 14 (1998) 6681.
[38] Z. Qu, W. Huang, M. Cheng, X. Bao, J. Phys. Chem. B 109 (2005) 15842.